Storage and Adiabatic Cooling of Polar Molecules in a Microstructured Trap

B. G. U. Englert, M. Mielenz, C. Sommer, J. Bayerl, M. Motsch,* P. W. H. Pinkse,† G. Rempe, and M. Zeppenfeld‡
Max-Planck-Institut für Quantenoptik, Hans-Kopfermann-Str. 1, D-85748 Garching, Germany
(Dated: July 15, 2011)

We demonstrate loading, trapping and adiabatic cooling of polar molecules in a new type of electric trap. The trap consists of two microstructured capacitor plates with an additional perimeter electrode, allowing for homogeneous fields in the trap volume and steep fields at the trap boundary. CH_3F molecules are trapped up to 60 seconds, with a $1/e$ storage time of 12 seconds. Applying different electric fields in two halves of the trap, adiabatic cooling is achieved by slowly expanding the trap volume. The trap is ideally suited for precision studies of ultracold molecular collisions and spectroscopy. Moreover, it combines all ingredients for the recently proposed opto-electrical molecular cooling scheme [M. Zeppenfeld et al., Phys. Rev. A 80, 041401(R) (2009)].

PACS numbers: 37.10.Mn, 37.10.Pq
Keywords: adiabatic cooling, cold molecules, electrostatic trapping

Precise control of the motional degrees of freedom of cold atoms has resulted in fundamental achievements in precision measurements and quantum technology. Compared to the previous focus on atomic systems, molecules offer novel possibilities due to additional internal degrees of freedom and strong long-range interactions. For example, cold molecules are promising candidates for precision tests of fundamental symmetries [1, 2], allow unique approaches to quantum computation [3, 4], offer new quantum-mechanical reaction channels [5, 6], and can condense to new quantum phases of matter [7, 8]. However, realizing a comparable degree of control over molecules as for atoms remains a challenge, mainly due to the general lack of fast optical cycling transitions. In this respect, it is advisable to make use of any advantages offered by molecules, in particular the strong interaction of dipolar molecules with electrostatic fields. A primary application for these interaction is the trapping of molecules [9–12]. By providing long interrogation times in a compact environment, electric traps hold great promise for fascinating applications [13–15]. Not least, a suitable electric trap is a key component of opto-electrical cooling [16], a general Sisyphus-cooling scheme for polar molecules.

In this Letter we present the experimental realization of a novel electric trap, featuring several key innovations. Specifically, molecules are trapped in a box-like potential where tunable homogeneous offset electric fields can be applied to a large fraction of the trap volume. High trapping fields exist only at the trap boundary. Homogeneous fields allow molecular transitions to be addressed by lasers or microwaves with strongly suppressed Stark broadening. Furthermore, an offset field in the central trap region greatly reduces the presence of field zeros, thereby suppressing losses via non-adiabatic transitions [17]. In fact, molecules are stored for up to a minute with a $1/e$ time of up to 12 seconds. To achieve such long storage times, the two trap outlets required for loading and unloading of the molecules are closed electrically. A unique feature of our trap is the subdivision into two trap regions where homogeneous electric fields can be applied independently. This allows for additional control of the motion of the molecules, which we demonstrate by cooling of the molecules via an adiabatic expansion in the trap.

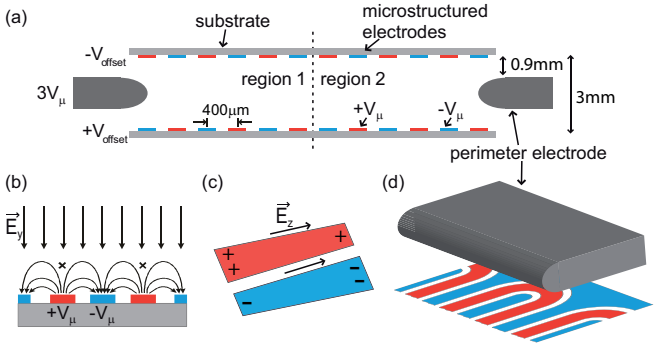

FIG. 1: (Color online). (a) Side view of the electric trap (not to scale). The trap consists of a high-voltage perimeter electrode and capacitor plates with microstructured surface electrodes. Trap dimensions are 4 cm × 2 cm × 3 mm. (b)-(d) Details of the electric-field configuration and microstructure electrode design as discussed in the text.

A schematic of the trap is presented in Fig. 1(a). Two parallel capacitor plates produce arbitrary homogeneous electric fields in a large fraction of the two trap regions 1 and 2. To prevent molecules from colliding with the plate surfaces, a planar array of equidistant ($400\,\mu$m) microstructured electrodes is deposited on the capacitor plates. Applying opposite-polarity voltages $\pm V_\mu$ to adjacent electrode stripes creates large repelling electric fields near the plate surfaces that exponentially decay away from the plates [18, 19]. Between the plates, a background field is produced by applying additional offset voltages $\pm V_{\rm offset}$ to the two plates. Transverse confinement of the molecules is achieved by a high-voltage electrode between the plates that surrounds the perime-

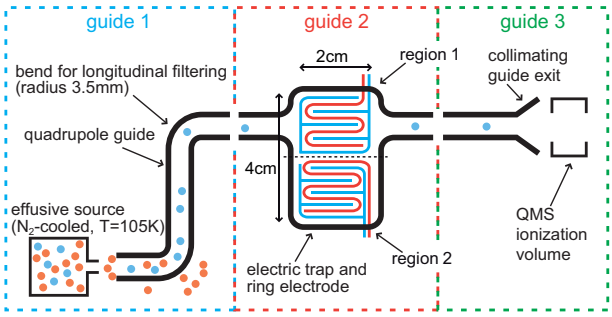

FIG. 2: (Color online). Schematic of the setup. The slowest molecules from a liquid-nitrogen-cooled reservoir are loaded into the electric trap via a quadrupole guide connected to the trap. For detection, an exit quadrupole guides the molecules to a quadrupole mass spectrometer (QMS).

ter of the trap.

To suppress trap losses, attention must be paid to the details of the electric fields. As shown in Fig 1(b), the interference of the microstructure field with a homogeneous offset field gives rise to a zero electric field (indicated by crosses in Fig. 1(b)) above every second microstructure electrode. These zeros cause trap losses in two ways: First, molecules are likely to undergo non-adiabatic transitions, so-called Majorana flips, to states that are no longer trapped [17]. Second, these zeros continue underneath the perimeter electrode, allowing molecules to leak out of the trap volume. To reduce Majorana flips, the microstructured electrode stripes are slightly wedged as shown in Fig. 1(c). This produces an additional component of the electric field E_z parallel to the stripes, thereby eliminating the electric field zero. To avoid "leaking" of the molecules from the trap, the microstructured electrodes with the same polarity as the perimeter electrode are interconnected under the perimeter electrode (Fig. 1(d)), causing the holes to lead back into the trap.

Operating the trap requires a suitable source of molecules and a means for their detection. This leads to an integration of the trap in the experimental setup as shown in Fig. 2. As a source of molecules we employ velocity filtering with an electric quadrupole guide from a liquid-nitrogen-cooled effusive nozzle as described in detail elsewhere [20]. This method has the advantage of providing a large continuous flux of molecules using a very robust setup. The geometry of the trap is specifically chosen to permit the connection to a quadrupole guide. Here, interrupting the perimeter electrode of the trap allows two opposing electrodes of the quadrupole guide to be connected to the trap. The other two electrodes of equal polarity merge with the microstructured plates. After trapping, the molecules are guided to the ionization volume of a quadrupole mass spectrometer (QMS), enabling time-resolved measurements. For signal enhancement, the guide electrodes at the exit of the guide are bent outwards which, similar to a microwave horn antenna, collimates the molecules onto the ionization volume of the QMS. Note that the guide used in our experiment consists of three independently switchable segments, allowing loading and unloading of molecules to be switched on or off without affecting the trapping fields.

Great care has been taken to ensure that the molecules experience a similar potential depth everywhere. In particular, this calls for appropriate voltage ratios to be applied to the various electrodes. For the maximum used electric field strength of $60\,\frac{\mathrm{kV}}{\mathrm{cm}}$, a voltage of $\pm V_\mu = \pm 1.8\,\mathrm{kV}$ is applied to the microstructure, whereas the perimeter electrode voltage and the voltage difference applied to the 1st and 3rd guide during trap loading and unloading is $V_{\mathrm{perimeter}} = 3V_\mu = 5.4\,\mathrm{kV}$. For a molecular state with an effective dipole moment of 1 D, this corresponds to a potential depth of $k_\mathrm{B} \times 1.45\,\mathrm{K}$. For other trap depths, all voltages are scaled accordingly.

The measurements are carried out with fluoromethane (CH_3F), a lightweight symmetric-top molecule, but in principle all molecules with significant Stark shifts can be used. The density of trapped CH_3F-molecules for the maximum trapping fields is approximately $10^8\,\mathrm{cm}^{-3}$, as has been determined via a QMS calibration [21]. Note that this value mainly reflects the density of molecules in the source.

For trap characterization, we first determined the trap lifetime by varying the holding time for molecules in the trap. Loading and unloading is carried out at reduced trap and guiding fields, allowing us to filter molecules with smaller velocities and efficiently extract these molecules, respectively. During the holding time the voltages are increased, resulting in a deep confinement for the loaded molecules. This leads to the following experimental protocol: Initially, molecules are continuously loaded into the trap for a time interval $t_{\mathrm{load}} = 3\,\mathrm{s}$ at a reduced confinement field E_{load}. This establishes a steady state in the trap. Measurements were performed for two loading fields, $E_{\mathrm{load}} = 20\,\frac{\mathrm{kV}}{\mathrm{cm}}$ and $E_{\mathrm{load}} = 30\,\frac{\mathrm{kV}}{\mathrm{cm}}$, corresponding to slower and faster molecules, respectively [20]. This allows us to analyze the dependence of the trap lifetime on the initial velocity distribution of the molecules. After the loading process, the trapping fields are increased to $E_{\mathrm{hold}} = 60\,\frac{\mathrm{kV}}{\mathrm{cm}}$ to confine the molecules in the trap during the holding time, t_{hold}, ranging from 1 to 60 s. During this time, high negative voltages are applied to the 1st and 3rd guide. This creates a repelling electric field at the gaps between the guides so that molecules that attempt to leave the trap via the entrance or exit guide are reflected back into the trap, thereby electrically closing the two outlets of the trap. After t_{hold}, the trap and the 3rd guide are switched back to a guiding configuration with $E_{\mathrm{unload}} = E_{\mathrm{load}}$ and the molecules are extracted from the trap during the unloading time $t_{\mathrm{unload}} = 3\,\mathrm{s}$.

Fig. 3(a) shows typical time-of-flight (TOF) signals for

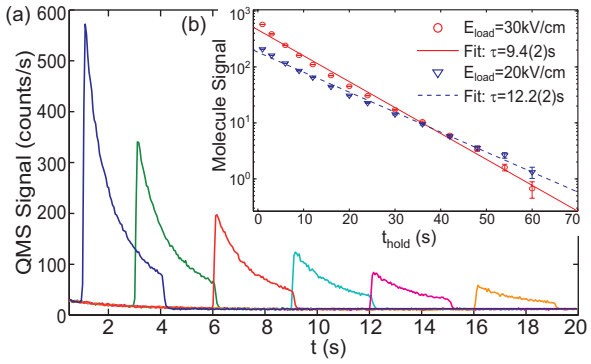

FIG. 3: (Color online). (a) Trap unloading signal for $E_{\mathrm{load}} = 30\,\frac{\mathrm{kV}}{\mathrm{cm}}$ and different holding times t_{hold} versus time t after closing the trap. (b) Integrated unloading signal of the molecules as a function of t_{hold} for two loading field strengths ($20\,\frac{\mathrm{kV}}{\mathrm{cm}}$ and $30\,\frac{\mathrm{kV}}{\mathrm{cm}}$). The blue (dashed) and the red (solid) line are exponential fits for the determination of the lifetime.

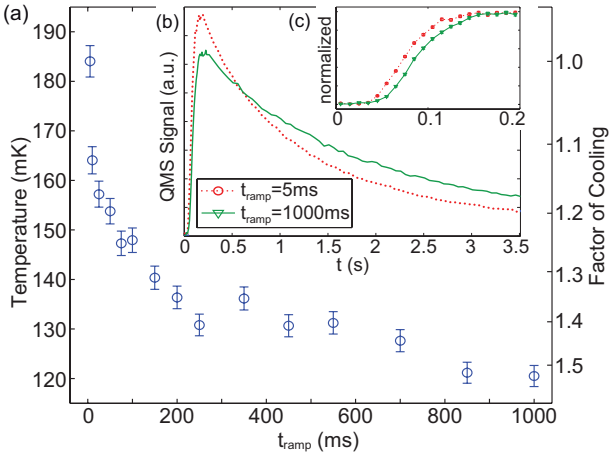

FIG. 4: (Color online). (a) Molecule temperature and cooling factor for the adiabatic cooling versus the ramping time. (b) Typical TOF signal. Molecules with $t_{\mathrm{ramp}} = 1000\,\mathrm{ms}$ arrive later and decay slower than molecules with $t_{\mathrm{ramp}} = 5\,\mathrm{ms}$. (c) Close-up of the normalized rising edge signal.

the unloading process for different holding times. Upon switching the 3rd guide to guiding configuration after t_{hold}, the QMS signal increases due to the arrival of molecules. This increase is followed by a slow decay as the number of molecules left in the trap decreases. In Fig. 3(b) the integrated molecule signal for the two different loading fields is plotted as a function of t_{hold}. As can be seen, even after $t_{\mathrm{hold}} = 60\,\mathrm{s}$ we still measure molecules from the trap. To determine the trap lifetime for slower ($E_{\mathrm{load}} = 20\,\frac{\mathrm{kV}}{\mathrm{cm}}$) and faster ($E_{\mathrm{load}} = 30\,\frac{\mathrm{kV}}{\mathrm{cm}}$) molecules, the data are fitted with an exponential decay function. Evidently, slower molecules have a longer trap lifetime which is consistent with Majorana flips being one of the main loss mechanisms for molecules in the trap. Additional contributions might be due to collisions with the background gas (the pressure is $\sim 1 \times 10^{-10}\,\mathrm{mbar}$ in the trap chamber) or remaining holes in the trap. Lastly, note that the data show slight deviations from the exponential decay function. This is due to a larger initial decay rate which is again consistent with faster molecules getting lost from the trap at a higher rate.

As a second test, we demonstrate the versatility of our trap by performing adiabatic cooling of the molecules. Here, the temperature is reduced by adiabatically expanding a molecular gas from one to both trap regions. This doubling of the trap volume is implemented by ramping down a potential step in the middle of the trap. As for the previous measurements, molecules are loaded into the trap during $t_{\mathrm{load}} = 3\,\mathrm{s}$ with $E_{\mathrm{load}} = 20\,\frac{\mathrm{kV}}{\mathrm{cm}}$. Subsequently all voltages are ramped up and an electric offset field of $20\,\frac{\mathrm{kV}}{\mathrm{cm}}$ is applied between the plates in region 1, creating a large potential step in the trap. Due to the large voltages, the confinement field between one of the plates in region 1 and the perimeter electrode is zero, causing all molecules not confined to region 2 to be lost from the trap during the emptying time $t_{\mathrm{empty}} = 500\,\mathrm{ms}$.

Next, the offset field in region 1 is ramped down to the offset field in region 2 in the ramping time t_{ramp}, thereby doubling the trap volume. This expansion process is expected to conserve the phase-space density of the molecules if it is done adiabatically. Therefore, in the experiment t_{ramp} is varied to analyze the timescale of adiabaticity; the subsequent holding time is chosen such that $t_{\mathrm{ramp}} + t_{\mathrm{hold}} = 1.1\,\mathrm{s} = \mathrm{const}$. Finally, molecules are unloaded during $t_{\mathrm{unload}} = 3.5\,\mathrm{s}$.

Figs. 4(b) and (c) compare the TOF unloading signal for the slowest ($t_{\mathrm{ramp}} = 1000\,\mathrm{ms}$) and fastest ($t_{\mathrm{ramp}} = 5\,\mathrm{ms}$) ramping; for these two cases the most significant signal difference is expected. As can be seen, for slower ramping of the electric fields the molecules arrive later at the QMS, demonstrating a slower velocity distribution. This is corroborated by the slower decay for the 1000 ms ramp since slower molecules have a lower trap loss rate as shown by the trap lifetime measurement. The overall number of measured molecules is even slightly higher for $t_{\mathrm{ramp}} = 1000\,\mathrm{ms}$ than for $t_{\mathrm{ramp}} = 5\,\mathrm{ms}$. This is clear evidence that the velocity reduction is not due to a filtering process but rather that a new, shifted velocity distribution is created by the ramping process.

We estimate the molecular temperature T for the different ramping times according to $k_{\mathrm{B}}T/2 = m\,\langle v_z\rangle^2/2$ from the rising edge of the normalized TOF signal $S(t)$. Here, $\langle v_z\rangle$ is the mean of the longitudinal velocity distribution $\rho(v_z)\mathrm{d}v_z$ in the exit guide which determines the normalized TOF signal. Noting that $S(t) = \int_{L/t}^{\infty} \rho(v_z)\mathrm{d}v_z$ with L being the length of the third guide, we find

$$\langle v_z\rangle = L \int_0^{\infty} \frac{1}{t^2} S(t)\,\mathrm{d}t. \qquad (1)$$

In addition to the temperature T, we define the cooling factor F for each ramping time as the ratio in T between the given ramping time and the fastest ramping time. The resulting values of T and F are shown in Fig. 4(a) as a function of the ramping time. As expected for a transition from a non-adiabatic to an adiabatic process, we see a steep initial increase of the cooling factor followed by a plateau. The transition between the two at $t_{\mathrm{ramp}} \approx 100\,\mathrm{ms}$ corresponds to a molecule with a typical velocity of 6 m/s traveling back and forth the full 4 cm length of the trap a total of maximally 8 times. Given the need for a molecule to switch regions several times for the process to be adiabatic, the frequent change in direction of a molecule upon reflection from the microstructure field and the need for the various velocity components to mix, this 100 ms timescale of adiabaticity therefore seems reasonable. For $t_{\mathrm{ramp}} = 1000\,\mathrm{ms}$ we determine a maximum cooling factor $F_{\mathrm{max}} = 1.53 \pm 0.03$, with the corresponding minimal temperature $T_{\mathrm{min}} = 121 \pm 2\,\mathrm{mK}$.

To estimate the yield of the adiabatic cooling we compare the experimental results with the maximum cooling factor we expect from theory. At first, molecules are only confined in trap region 2. When the initial kinetic energy of the molecules exceeds the potential barrier due to the high electric fields in region 1, the molecules can enter this region where they lose energy due to the potential step. If this expansion of the molecular gas to double its volume is done adiabatically, the phase-space density is conserved and the molecular temperature is reduced by a theoretical factor of $F_{\mathrm{opt}} = 2^{2/d}$, with $d = 3$ being the spatial degree of freedom of the contributing velocities. Comparing this theoretically expected maximum cooling factor $F_{\mathrm{opt}} = 1.59$ to the experimentally measured value results in an experimental yield of $\log(F_{\mathrm{max}})/\log(F_{\mathrm{opt}}) = 92 \pm 3\%$. The main limitation in the experiment is given by the non-zero ramping time of the fastest ramping which is used as the non-adiabatic reference point T_{max} for all data points. Faster ramping than 5 ms could result in the demonstration of even higher yields, but is hard to implement due to technical limitations of our voltage supplies.

In summary, we have presented the first experimental demonstration of a microstructured box-like electric trap with adjustable homogeneous offset fields. Molecules are stored for up to 60 s with a trap lifetime of $12.2 \pm 0.2\,\mathrm{s}$ which, to our knowledge, is the longest lifetime shown for an electric trap to date. Additionally, adiabatic cooling has been demonstrated with a cooling factor of up to 1.53 ± 0.03 corresponding to a cooling yield of at least $92 \pm 3\%$. This controlled microstructure-based manipulation of molecules is a major step towards scalable trapping systems as in atom chip experiments [22].

Notwithstanding the excellent performance of the trap, further improvements are possible. For example, non-adiabatic transitions as one of the main loss mechanisms can be suppressed by better tailoring the microstructure electrodes. The density of molecules in the trap can be increased by combining the trap with, e.g., velocity filtering from a cryogenic buffer-gas cooled source [21] or via laser-induced accumulation of molecules inside the trap [16]. Further increasing the electrode voltages also increases the density.

Already the present trap enables a number of measurements. For example, the addition of suitable microwave and optical fields will allow cooling of both the motional and the internal degrees of freedom of polar molecules [16, 23, 24]. Homogeneous offset fields and the long trap lifetime can be used for precision Stark spectroscopy [25] or the investigation of weak transitions [13]. Finally, tuning of the offset field will allow field-induced collision resonances to be investigated [14].

We acknowledge support by the Deutsche Forschungsgemeinschaft through the excellence cluster "Munich Centre for Advanced Photonics".

* Present address: Laboratorium für Physikalische Chemie, ETH Zürich, CH-8093, Switzerland
† Present address: MESA+ Institute for Nanotechnology, University of Twente, 7500AE, The Netherlands
‡ Electronic address: martin.zeppenfeld@mpq.mpg.de

[1] E. A. Hinds, Phys. Scr. **T70**, 34 (1997).
[2] J. J. Hudson *et al.*, Nature **473**, 493 (2011).
[3] D. DeMille, Phys. Rev. Lett. **88**, 067901 (2002).
[4] A. André *et al.*, Nat. Phys. **2**, 636 (2006).
[5] R. V. Krems, Phys. Chem. Chem. Phys. **10**, 4079 (2008).
[6] P. S. Zuchowski and J. M. Hutson, Phys. Rev. A **79**, 062708 (2009).
[7] K. Góral, L. Santos, and M. Lewenstein, Phys. Rev. Lett. **88**, 170406 (2002).
[8] A. Micheli, G.K. Brennen, and P. Zoller, Nat. Phys. **2**, 341 (2006).
[9] S. Y. T. van de Meerakker *et al.*, Phys. Rev. Lett. **94**, 023004 (2005).
[10] T. Rieger *et al.*, Phys. Rev. Lett. **95**, 173002 (2005).
[11] J. Kleinert *et al.*, Phys. Rev. Lett. **99**, 143002 (2007).
[12] S. D. Hogan, Ch. Seiler, and F. Merkt, Phys. Rev. Lett. **103**, 123001 (2009).
[13] S. Y. T. van de Meerakker *et al.*, Phys. Rev. Lett. **95**, 013003 (2005).
[14] A. V. Avdeenkov and J. L. Bohn, Phys. Rev. A **66**, 052718 (2002).
[15] M. R. Tarbutt *et al.*, Faraday Discuss. **142**, 37 (2009).
[16] M. Zeppenfeld *et al.*, Phys. Rev. A **80**, 041401(R) (2009).
[17] M. Kirste *et al.*, Phys. Rev. A **79**, 051401 (2009).
[18] S. J. Wark and G. I. Opat, J. Phys. B **25**, 4229 (1992).
[19] S. H. Schulz *et al.*, Phys. Rev. Lett. **93**, 020406 (2004).
[20] T. Junglen *et al.*, Eur. Phys. J. D **31**, 365 (2004).
[21] C. Sommer *et al.*, Faraday Discuss. **142**, 203 (2009).
[22] A.D. Cronin, J. Schmiedmayer and D.E. Pritchard, Rev. Mod. Phys. **81**, 1051 (2009).
[23] I. S. Vogelius, L. B. Madsen and M. Drewsen, Phys. Rev. Lett. **89**, 173003 (2002).
[24] G. Morigi *et al.*, Phys. Rev. Lett. **99**, 073001 (2007).
[25] M. Motsch *et al.*, Phys. Rev. A **76**, 061402(R) (2007).